C. R. Mecanique 347 (2019) 863–872

Contents lists available at ScienceDirect

Comptes Rendus Mecanique

www.sciencedirect.com

Data-Based Engineering Science and Technology / *Sciences et technologies de l'ingénierie basées sur les données*

Modal decomposition from partial measurements

Clément Jailin [a,b], Stéphane Roux [a,*]

[a] *LMT (ENS Paris-Saclay/CNRS/Université Paris-Saclay), 61, avenue du Président-Wilson, 94235 Cachan, France*
[b] *Safran Tech, rue des Jeunes-Bois, 78772 Magny-les-Hameaux, France*

ARTICLE INFO

Article history:
Received 3 August 2019
Accepted after revision 10 August 2019
Available online 14 November 2019

Keywords:
Modal analysis
Proper generalized decomposition
Dynamic stereo-vision
Dynamic tomography
Field recovery
Gappy proper orthogonal decomposition

ABSTRACT

A data set over space and time is assumed to have a low-rank representation in separated spatial and temporal modes. The problem of evaluating these modes from a temporal series of *partial measurements* is considered. Each elementary instantaneous measurement captures only a "window" (in space) of the observed data set, but the position of this window varies in time so as to cover the entire region of interest and would allow for a complete measurement would the scene be static. A novel procedure, alternative to the Gappy Proper Orthogonal Decomposition (GPOD) methodology, is introduced. It is a fixed-point iterative procedure where modes are evaluated sequentially. Tested upon very sparse acquisition (1% of measurements being available) and very noisy synthetic data sets (10% noise), the proposed algorithm is shown to outperform two variants of the GPOD algorithm, with much faster convergence, and better reconstruction of the entire data set.

1. Introduction

In experimental mechanics, full-field measurements are an essential ingredient for the identification and validation of mechanical laws. Initially developed for 2D plane measurements with Digital Image Correlation, (DIC) [1], and extended to stereo-correlation [2] and 3D analyses (Digital Volume Correlation, DVC [3]), they provide rich data to challenge complex models or to feed data-driven approaches. Performed *in-situ* (*i.e.* during a mechanical test), the recent evolution of those approaches to space-time measurements (both for 2D [4] and 3D [5]) provided an enhanced sensitivity fostering the identification of strongly non-linear behaviors. Therefore, acquiring a complete set of *in situ* space and time measurements is a grail in experimental mechanics.

However, the acquisition of a *complete* stack of data is generally inaccessible. Incomplete acquisition, in a mechanical context, can be due to many reasons and to mention just of few of them:

- intrinsically incomplete measurement devices (*e.g.*, mobile camera imaging a large or curved surface [6], partial space-time measurements in a Continuous Scanning Laser Vibrometer (CSLV) [7], etc.);
- partially masked field of view, either unwanted (*e.g.*, due to the experimental setup [8]) or voluntary (*e.g.*, because of the detector saturation of a part of the sample due to specular reflection in [9] or due to the degradation of the imaged texture and speckles [10]);

* Corresponding author.
E-mail addresses: clement.jailin@ens-paris-saclay.fr (C. Jailin), stephane.roux@ens-paris-saclay.fr (S. Roux).

https://doi.org/10.1016/j.crme.2019.11.011

- fast rate phenomena that can be studied with an acquisition rate that is too low. This problem can be circumvented if the exploited image is processed from the fast acquisition of a collection of raw data (*e.g.*, in computed tomography, MRI, diffraction patterns in EBSD, etc.). In tomography, while 3D measurements require the (very) long acquisition time of volumes, the development of projection-based measurement methods [11,12] made it possible to image fast phenomena. As they are based on projection and not on volumes, these methods exploit, at each time/loading step, only a partial (projected) spatial information;
- an intentionally sparse acquisition aiming at a reduction of data storage and processing.

Although incomplete, other modalities/sensors are often coupled with full-field measurements as they provide complementary information (generally continuous in time and sparse in space) such as load measurements, extensometers, impedance measurements, etc.

In mechanical tests, the measurement of the kinematics is generally based on highly redundant (yet noisy) data [13] (*e.g.*, refer to the 6050 (2048×2048 pix) images acquired in [9]). Moreover, those space-time measurements are themselves also redundant when dealing with model identification. Hence, a natural trend to perform fast experiments and to tolerate noisy data is to investigate the possibility to deal with as little information as possible. Namely, having a way to deal efficiently with a sparse support in space and or time for the measurement would be highly desirable.

Field recovery from measurements with missing data or data corruption is addressed in a very abundant and diverse literature relevant to various fields. Different categories can be highlighted, such as

1) assumptions on the low rank of the recovered field, which lead to the determination of few modes composed of space and time functions. Such is the case, *e.g.*, in robust-Principal Component Analysis (PCA) [14,15], where a low-rank dynamic background corrupted by sparse defects may be cleaned assuming few modes;
2) methods based on *a priori* knowledge. In model-based measurements (called Integrated-DIC [16,17,5]), the displacement field is expressed from a model driven by a (partially-known) behavior. In previously introduced projection-based methods [12,18], an incomplete data set is supplemented by assumptions regarding the smooth temporal evolution. When the knowledge is on the variable statistics, optimal interpolation methods, as kriging, can be carried out;
3) approaches based on regularization penalties (l_1-norm and nuclear norm being the most popular in Compressed-Sensing [19,15], *e.g.*, applied for the image reconstruction of single-pixel cameras [20]);
4) other methods, based on prior full analyses (*e.g.*, Gappy-POD, Gappy-PCA, (GPCA) for the recovery of images [21] and fields [22,23]) allow recovering the complete field from learned dictionaries;

- in the first category (robust-PCA), data corruption is assumed to be sparse, whereas we are motivated by the opposite limit where reliable measurement is sparse;
- in the second approach, regularity assumptions issued from a physical model, or from an *a priori* assumption (as for Kriging), allows one to swiftly interpolate from known data to fill missing patches. This category can be seen as the use of an appropriate filter. Although efficient and physically sound, such approaches are discarded from the present analysis to address the very question of incompleteness, but they can be easily merged with the proposed methodology to supplement it with a specific filter;
- in the third approach (Compressed Sensing), the sought information (after possibly an appropriate transformation...) is assumed to have a sparse support, and it is this sparsity that is exploited to retrieve the information. For instance, when an image contains few phases, boundaries, being the support of non-zero gradients of the image, are sparse, and hence a total variation may be used to enforce a limited number of phases;
- in the fourth approach, Gappy-PCA (as PCA itself) does not necessitate any regularity assumption, although it is easy (and beneficial when relevant) to supplement them with a specific filter. This is so common that it is difficult to apprehend what contributes to the success of GPCA when both the PCA methodology and a regularizing filter are both present. In the present study, the choice is made to exclude all filters, or any recourse to continuity, to differentiability or even to low power of high frequencies. Thus, even if space and time are referred to, they may be thought of as disconnected positions in space and instant in time, which can be arbitrarily reshuffled either in space or in time. Hence, time is to be seen as a mere discrete labeling of the measurement instant, and space is equally a labeling of discrete position. Hence, the focus is made only on the sparsity of the measurement. Nevertheless, it is obviously needed that the number of measurements is somewhat larger than the information content of the exploited signal, the low information content (compatible with the sparse measurement) lies in the low rank of separated mode representation of the signal. The latter is indeed robust with respect to any permutation in space or in time. In such a context, GPCA is the reference methodology. In the present study, a variant algorithm is introduced, which provides similar or better results, with fewer iterations, in the limit of very sparse and noisy data.

Different measurement methods in mechanics have been developed to exploit this low rank of separated mode representation. Such is the case for vibration measurements [24] and also for quasi-static behaviors for the measurement [12] and identification [18] and ultra-fast dynamics with a crack propagation [25]. Inspired from the Proper Generalized Decomposition (PGD) technique [26], PGD–DIC consists of a progressive enrichment of the space-time modes for displacement corrections. As a side remark, those modal full field measurement methods were initially applied for the decomposition of

the different direction of the space displacements [24,27]. As such, PGD algorithms can be seen as a complete Gappy-POD method with the progressive modal identification.

After a presentation of the treated problem in section 2, the proposed method is described and discussed in section 3. Then, various applications are carried out to challenge the approach considering different measurement protocols and noises. The comparison with Gappy-POD methods is finally shown and highlights the efficiency of the proposed procedure.

2. Addressed problem

2.1. Notations

A space-time phenomenon is characterized by a physical quantity (which can be of any nature) whose space $\boldsymbol{x}$ and time t expression is denoted $A(\boldsymbol{x},t)$, which is discretized in space and time and represented as a matrix $A_{a\alpha}=A(\boldsymbol{x}_a,t_\alpha)$. Conventionally, in the following, Latin (resp. Greek) indices will refer to space (resp. time). This field is assumed to be well represented by an expansion over space-time modes,

$$A_{a\alpha}=\sum_{i=1}^{n} f^i\varphi^i_\alpha\Phi^i_a \tag{1}$$

where, conventionally, it is chosen to normalize all space Φ^i and time φ^i modes to unity, $\|\Phi^i\|_a=1$ and $\|\varphi^i\|_\alpha=1$, and hence f_i is the amplitude of mode i.

The field $A_{a\alpha}$ is unknown, but it is studied through different measurement devices. The measurement device acting at time t_α, is defined as a linear operator, $[\boldsymbol{M}_\alpha]$, which extracts from the field $A_{a\alpha}$, a set of measurements gathered in a vector $B_{a\alpha}=[\boldsymbol{M}_\alpha]_{ab}A_{b\alpha}$. Although the problem could easily be generalized, measurements are assumed instantaneous. A measurement is said to be "partial" if $[\boldsymbol{M}_\alpha]$ is rank deficient and cannot be inverted (the entire field $A_{\bullet\alpha}$ cannot be obtained from the snapshot $B_{\bullet\alpha}$). Additionally, in the following, the measurements B are polluted by a random Gaussian noise, characterized by its variance σ. An arbitrary spatial covariance matrix could be considered, using its inverse as the optimal metric tensor. For the sake of simplicity, noise will be considered as white (or spatially uncorrelated).

An example of such partial measurement is provided by a 3D phenomenon captured from a 2D detector. Inasmuch as one individual measurement device is incomplete, a full experiment consists in combining such partial measurements in time from different points of view, so that the 3D consistency can be captured. For instance, using stereo-vision, one can access 3D shape measurements making the combination of two (or several) partial measurement devices (2D cameras) a complete system. In the similar case of radiography, the combination of a (potentially large) number of projection directions allows the entire 3D microstructure to be reconstructed, provided the studied object remains still during the scan rotation, a process known as tomography.

Another trivial example of such partial measurements is such that, at each instant of time t_α, $[\boldsymbol{M}_\alpha]$ is simply the identity restricted to a limited set of points $\Omega(t_\alpha)$. In this case, $[\boldsymbol{M}_\alpha]=[\boldsymbol{I}]_{\Omega(t_\alpha)}$ is a diagonal matrix (projection over $\Omega(t_\alpha)$). In the following, this elementary case will be considered as a toy problem to investigate the retrieval of A from B, where the collection of data along time will supplement the partial measurement at each elementary instant, and exploit the property that only few space-time modes are sufficient.

This example is chosen so as to focus on the key point of compensating for lacking data, and not on the specific particularities of the measurement operator $[\boldsymbol{M}_\alpha]$.

In space and time, Fig. 1 shows several examples of partial measurements in space and time, for a rather low coverage. Often, measurements occur over a compact support ("window") that appears here as intervals. It is chosen here to consider intervals of the same length at each instant of time; however, the position of this set of measurements may move over time in discrete steps, in a regular fashion, and randomly. Those examples are representative of different acquisition strategies encountered in practice. The first case is encountered in the Scanning Laser Vibrometry technique [28]), or for the modal analysis of a vibrating object from radiographs acquired at few directions [29]. The second case illustrates the projection-based measurement methods [12], in which the projection of the sample is imaged during rotation and loading. Another application for the same case is the *Continuous* Scanning Laser Vibrometry techniques [7]. The third case is met when the window motion is erratic, as for instance for random acquisition patterns of the single-pixel camera [20].

In the limit of a very sparse acquisition, the question of invertibility will be discussed in the following. Eventually, an additional information, coming from additional sensors (generally continuous in time and local in space) such as load measurements, can be included to make the problem well-posed.

2.2. Static problem

Before addressing the modal analysis, let us specify our notations and recall how a *static* problem would be characterized optimally with respect to the set of noisy measurements.

The following cost function is introduced,

$$\mathcal{T}=(1/2)\sum_\alpha \|[\boldsymbol{M}_\alpha]\{\boldsymbol{A}_\alpha\}-\{\boldsymbol{B}_\alpha\}\|^2 \tag{2}$$

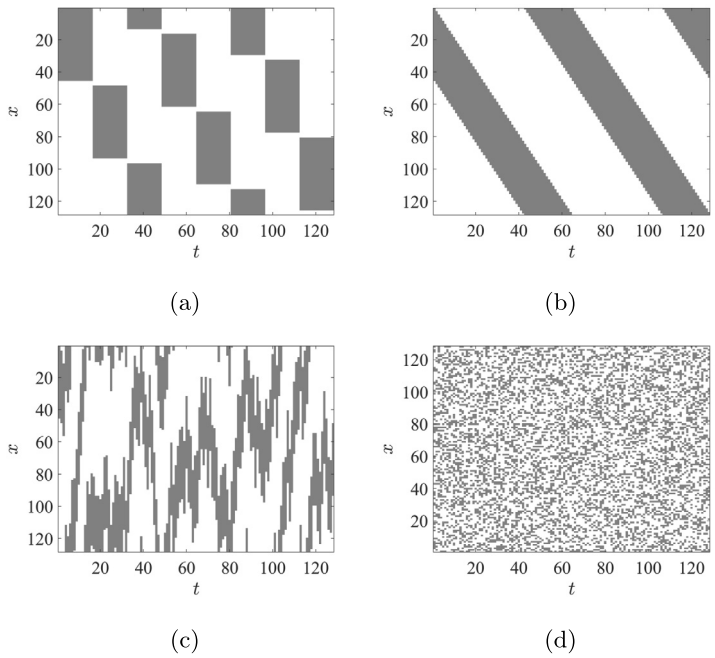

Fig. 1. An illustration of different partial measurements in space x and time t in the simple case of an indicator (shown in grey), for stepwise scan (a), continuous scan (b), randomly moving window (c), and random acquisitions (d). Here, for the sake of illustration, a large fraction of possible measurements has been chosen, $\eta = 35\%$, while in the test cases chosen in section 4, $\eta = 1\%$.

where the sought field and measurement in space at each instant t_α are gathered into a vector $\{\boldsymbol{A}_\alpha\}$, and the norm is the one resulting from a maximum likelihood based on noise covariance, **Cov**,

$$\|\{\boldsymbol{X}\}\|^2 \equiv \{\boldsymbol{X}\}^\intercal \cdot \left[\mathbf{Cov}^{-1}\right] \cdot \{\boldsymbol{X}\} \tag{3}$$

For the white noise considered herein, this norm reduces to the Euclidian (L2) one.

Minimizing the cost function with respect to $\{\boldsymbol{A}\}$ leads to

$$\sum_\alpha [\boldsymbol{M}_\alpha]^\intercal \left([\boldsymbol{M}_\alpha]\{\boldsymbol{A}_\alpha\} - \{\boldsymbol{B}_\alpha\}\right) = 0 \tag{4}$$

or

$$\sum_\alpha \left([\boldsymbol{M}_\alpha]^\intercal [\boldsymbol{M}_\alpha]\right) \cdot \{\boldsymbol{A}_\alpha\} = \sum_\alpha [\boldsymbol{M}_\alpha]^\intercal \{\boldsymbol{B}_\alpha\} \tag{5}$$

Let us define $[\mathcal{H}_\alpha] = [\boldsymbol{M}_\alpha]^\intercal [\boldsymbol{M}_\alpha]$ and $[\boldsymbol{H}]$:

$$[\boldsymbol{H}] \equiv \sum_\alpha [\mathcal{H}_\alpha] \tag{6}$$

It is this matrix, discussed in the introduction of section 2, that has to be inverted, whereas $[\mathcal{H}_\alpha]$ cannot be as it is rank deficient. The sum over α allows all complementary measurements to participate to the identification. The minimizer of $\mathcal{T}$ then reads

$$\{\boldsymbol{A}_\alpha\} = [\boldsymbol{H}]^{-1} \cdot \left(\sum_\alpha [\boldsymbol{M}_\alpha]^\intercal \{\boldsymbol{B}_\alpha\}\right) \tag{7}$$

3. Proposed algorithm

Let us first recall the basic principle of the GPOD algorithm [21], and a variant of it [30].

GPOD relies on a plain POD algorithm, applied to a complete set of data. However, because some data are lacking, fake values are used over this missing part. To initiate the process, an average value of the known data is used to fill in those parts, where averages may be computed over time or space or both [21]. POD is run over the resulting data set, with a specified number of modes. Then, the same procedure is repeated after data completion with the identified modes, and

keeping the actual measurements unchanged. Upon iterations, the missing parts are progressively filled with data that are more and more consistent with the measured ones. The procedure is stopped when a stationary solution has been reached. This algorithm will be referred to as GPOD1. There exist variants of this algorithm that are faster but approximate and they are not discussed herein.

Let us however mention a variant—hereafter referred to as GPOD2—such that the number of modes is not fixed for the entire procedure. On may run the same GPOD1 procedure, searching for one single mode to start with. After convergence, the number of sought modes is incremented up to the desired value (or after the incremental benefit of using an additional mode is not considered sufficient). The resulting modes obtained with this variant is similar to the previous (when the problem admits a unique solution) because the last iteration loop is similar, but convergence is faster [30].

Let us stress that the beauty of the GPOD algorithms is to turn an absence of measurement into a "fake" one, but where the alleged "measured" value is tuned to be the least inconsistent with the actual ones. This substitutes to each Hessian $[\mathcal{H}_\alpha]$, a "completed" one that restores invertibility and makes the identification from each measurement instant a well-posed problem.

3.1. Proposed algorithm

As for GPOD2 procedure, the initial step is to identify a *single* mode. However, in contrast to the above two algorithms, missing data are not fudged, even temporarily. When no measurement is performed, no extraneous equation is introduced.

From a set of measurements, $\{\boldsymbol{B}_\alpha\}$, one looks for the spatial mode $\{\boldsymbol{\Phi}\}$, the temporal function φ_α and amplitude γ such that the following cost function is minimized

$$\mathcal{T}(\{\boldsymbol{\Phi}\},\{\boldsymbol{\varphi}\}) = (1/2)\sum_\alpha \|\gamma\varphi_\alpha[\boldsymbol{M}_\alpha]\{\boldsymbol{\Phi}\} - \{\boldsymbol{B}_\alpha\}\|^2 \tag{8}$$

under two additional normalization conditions $\langle\varphi_\alpha^2\rangle_\alpha = 1$, and $\langle\Phi_a^2\rangle_a = 1$. Thus, one has to solve the following two equations, Eqs. (9) and (10).

$$\{\boldsymbol{\Phi}\} = \underset{\{\boldsymbol{\Phi}^*\}}{\text{Argmin}}\ \mathcal{T}(\{\boldsymbol{\Phi}^*\},\{\boldsymbol{\varphi}\}) \tag{9}$$

$$\varphi(t) = \underset{\{\boldsymbol{\varphi}^*\}}{\text{Argmin}}\ \mathcal{T}(\{\boldsymbol{\Phi}\},\{\boldsymbol{\varphi}^*\}) \tag{10}$$

On the one hand, the minimization of $\mathcal{T}$ with respect to $\{\boldsymbol{\Phi}^*\}$, leads to

$$\gamma\left(\sum_\alpha \varphi_\alpha^2[\boldsymbol{M}_\alpha]^\intercal[\boldsymbol{M}_\alpha]\right)\cdot\{\boldsymbol{\Phi}\} = \sum_\alpha \varphi_\alpha[\boldsymbol{M}_\alpha]^\intercal\{\boldsymbol{B}_\alpha\} \tag{11}$$

On the other hand, the determination of the associated temporal amplitudes is obtained by a minimization of $\mathcal{T}$ with respect to φ_α, giving

$$\gamma\varphi_\alpha = \frac{\{\boldsymbol{\Phi}\}^\intercal[\boldsymbol{M}_\alpha]^\intercal\{\boldsymbol{B}_\alpha\}}{\{\boldsymbol{\Phi}\}^\intercal[\mathcal{H}_\alpha]\{\boldsymbol{\Phi}\}} \tag{12}$$

It is proposed to use a fixed-point algorithm, where φ_α is first initialized to 1, and, from Eq. (11), $\gamma\{\boldsymbol{\Phi}\}$ is computed. The spatial mode and its amplitude are then obtained from their product by using the normalization condition $\langle\Phi_a^2\rangle_a = 1$. Then, from the determined spatial mode, the temporal evolution, $\gamma\{\boldsymbol{\varphi}\}$, is computed from Eq. (12), and again, γ is determined by the normalization condition $\langle\varphi_\alpha^2\rangle_\alpha = 1$. The staggered determination of the spatial and temporal modes is iterated until a fixed point is reached. This concludes the determination of the first (dominant) POD mode.

As for PGD methods, the measurement is performed by adding modes progressively, one at a time. Once a first mode is measured, a residual, expressed only on the measured areas, is computed as

$$\{\boldsymbol{R}_\alpha\} = \{\boldsymbol{B}_\alpha\} - \gamma\varphi_\alpha[\boldsymbol{M}_\alpha]\{\boldsymbol{\Phi}\} \tag{13}$$

This residual $\{\boldsymbol{R}_\alpha\}$ is substituted to the measurement data, $\{\boldsymbol{B}_\alpha\}$, in the above "single-mode" procedure, providing the second mode, which is subtracted from the starting data to give a second residual. The latter substitution of successive residuals is iterated to generate as many modes as needed until the residual is comparable to noise.

It is to be underlined that the solution to Eq. (9) never involves "fake" measurements. As compared to GPOD, where the latter are included to restore invertibility at each instant of time, they also endow the algorithm with a kind of "inertia," that slows down convergence. Thus the proposed algorithm is expected to show a much faster convergence. Yet, in the absence of noise, all those algorithms should converge toward the same (exact) solution. For noisy data, the proposed scheme that always gives the proper weight to each measurement is expected to be more robust.

It is to be noted that such a greedy approach for the case of complete measurements is strictly equivalent to the plain POD approach, where all modes are sought simultaneously. In the following, because of our choice of considering a toy

problem for which the metric is just trivial, PCA, POD or PGD are three different names for an equivalent result. However, it is to be observed that, when the norm used in the functional to be minimized results from an arbitrary variational formulation, (a PGD-type problem), the very same procedure can be duplicated, providing the corresponding generalization to sparse data acquisition. Just to mention a simple example, when noise is spatially correlated, the introduction of a metric based on the inverse covariance matrix (see Eq. (3)) is trivially taken into account in the above cost function, and it would prevent a straightforward use of GPOD.

3.2. Uniqueness for one single mode

Let us now consider the particular case of the toy model of direct measurements, $[\boldsymbol{M}_\alpha] = [\boldsymbol{I}]_{\Omega(t_\alpha)}$. Thus, $[\boldsymbol{H}] = \sum_\alpha [\boldsymbol{M}_\alpha]^2 = \sum_\alpha [\boldsymbol{M}_\alpha]$ is also diagonal and the ath element along the diagonal is $d_a = \sum_\alpha \mathcal{I}^\alpha(a)$, or, in other words, the number of times position a has been measured. Hence, the only condition for being able to invert the Hessian $[\boldsymbol{H}]$ is that all sites should be visited at least once. Obviously, this condition guarantees the uniqueness of the solution for the static case (where $\varphi_\alpha = 1$). More generally, when only one spatio-temporal mode is present, but the time evolution is not constant, then it is needed that all positions in space are visited at least once, but similarly along the time axis, at all considered instants, at least one measurement has been performed.

However, assessing uniqueness of the mode determination requires a more complete discussion. Let us consider the case of two batches of measurements, with, for instance, a first half of sites being measured during a first period of time, after what the second half is measured over the same amount of time. The first domain is labeled (X) and the second (Y). These two domains correspond to a natural partition in two sub-problems, each of which is solved by a standard POD. Considered globally, this problem is within the class of partial measurements. Let us suppose that this problem has been solved and that a mode has been computed

$$A_{a\alpha} = \gamma^{(1)} \varphi_\alpha^{(1)} \Phi_a^{(1)} \tag{14}$$

We can now construct another triplet $(\gamma^{(2)}, \boldsymbol{\varphi}^{(2)}, \boldsymbol{\Phi}^{(2)})$ such that

$$\begin{aligned} \varphi_\alpha^{(2)} &= \begin{cases} \omega_X \varphi_\alpha^{(1)} & \text{when} \quad \alpha \in (X) \\ \omega_Y \varphi_\alpha^{(1)} & \text{when} \quad \alpha \in (Y) \end{cases} \\ \Phi_a^{(2)} &= \begin{cases} (\lambda/\omega_X) \Phi_a^{(1)} & \text{when} \quad a \in (X) \\ (\lambda/\omega_Y) \Phi_a^{(1)} & \text{when} \quad a \in (Y) \end{cases} \end{aligned} \tag{15}$$

Let us define $\xi^2 = \|\varphi^{(1)}\|^2_{(X)}$ and $\eta^2 = \|\Phi^{(1)}\|^2_{(X)}$. In order to fulfill the normalization conditions of $(\varphi^{(2)}, \Phi^{(2)})$, the following two conditions are to be met

$$\begin{aligned} \omega_X^2 \xi^2 + \omega_Y^2 (1 - \xi^2) &= 1 \\ (\lambda/\omega_X)^2 \eta^2 + (\lambda/\omega_Y)^2 (1 - \eta^2) &= 1 \end{aligned} \tag{16}$$

Provided these two conditions are satisfied, $(f^{(2)}, \varphi^{(2)}, \Phi^{(2)})$ is just equivalent to $(f^{(1)}, \varphi^{(1)}, \Phi^{(1)})$; however, two conditions to determine three degrees of freedom λ/ω_X is lacking a constraint. Thus, the solution cannot be unique. Hence, although all observables B may be accounted for as a single space-time mode (one separated representation), the solution is not unique if no overlap between the measurement domains exist. This solution can be further extended to a collection of blocks with no overlap. Note, however, that overlap is to be considered after an arbitrary permutation of measurement of sites or instants. To evaluate the degeneracy of the solution in terms of modes, it suffices to count the number of connected components using simple graph-cut algorithms.

Furthermore, let us note that the connectedness of the components is not yet the ultimate criterion: if the connectedness of a single component is only due to a unique measurement at a particular location $\tilde{a}$ and time $\tilde{\alpha}$, its value may be seen as providing the additional equation needed to complement Eq. (16) enforcing $\omega_X = \omega_Y = \lambda = 1$. However, this necessitates that the value of the mode at this specific site and time, $\varphi_{\tilde{\alpha}}^{(1)} \Phi_{\tilde{a}}^{(1)}$, is not zero. This implies that the uniqueness of the solution is not only due to the measurement set-up (the choice of measurement positions and instants), but also to the modes that are measured. In particular, the locations where the mode vanishes (or simply assumes a low absolute value as compared to the surrounding) are potential sources of "fragility" for the solution. Those situations are typically those that are easily cured by requiring a smooth behavior for both spatial mode and/or time function.

As an alternative to having an overlap, let us note that adding an additional information may allow one to recover a well-posed problem. One natural assumption is that stationary modes are present, *e.g.*, because a vibrating system is subjected to a random but steady excitation [31,29]. In such a situation, possibly a wealth of information may be accessible (exploiting a statistical distribution that may be Gaussian), but the most robust ones rely on low-order statistical moments of the distribution per block, *i.e.* having an equal total "power" per block of measurements, $\langle \varphi_\alpha^2 \rangle_{\text{block}} = 1$ (similar to the global normalization). This implies only that the number of measurements is large per block as the decay of fluctuations (law of large numbers) is slow.

Table 1
Comparison for different test cases (Step scan, Continuous scan, Randomly moving scan, and Random acquisition) of the three algorithms (GPOD1, GPOD1, Present Method). For each combination of test case and algorithm, the number of iterations at convergence is given, together with the relative error at the end of the computation.

Case	Algorithm	Iterations	Final Error
Step scan	GPOD1	400*	0.024
Step scan	GPOD2	1240	0.020
Step scan	Present Method	198	0.019
Cont. scan	GPOD1	124	0.047
Cont. scan	GPOD2	116	0.049
Cont. scan	Present Method	30	0.024
Rand. mov. scan	GPOD1	99	0.042
Rand. mov. scan	GPOD2	192	0.040
Rand. mov. scan	Present Method	36	0.022
Random	GPOD1	334	0.054
Random	GPOD2	552	0.032
Random	Present Method	37	0.024

3.3. Uniqueness in the case of multiple modes

When multiple, N_{mode}, space-time modes are present, one may generalize the previously mentioned graph theoretic argument based on connected components. However, at least N_{mode} common sites should be shared between blocks so as to be considered connected.

The above discussion of uniqueness may be further extended to the analysis of uncertainty. Thus rather than just a determination of the well-posedness of the problem, an assessment of the uncertainties may reveal ghosts of the above undeterminations. The least stable eigenmodes may display such block-like multiplicative features as those analyzed above. This is what was indeed observed in test cases, especially when spatial and temporal modes crossed a 0 value. This point emphasizes the property that stability is not only a matter of experimental design, but also involves the properties of the observed modes. This observation was the motivation for introducing the previous discussion.

4. Test cases

The procedure is applied for the recovery of different synthetic test cases.

In order to test the proposed method, we chose extreme cases of sparse acquisition representing $\eta = 1\%$ of the entire $(\boldsymbol{x}, t)$ domain, where the latter is chosen to be of size $N_x = 1024$ locations in space and $N_t = 1024$ instants of time for measurements. Therefore, the number of measurements is $\eta N_x N_t$. Moreover, an additional Gaussian white noise is added to the measured data, with a standard deviation that represents 10% of the standard deviation of the reference data. (The signal-to-noise ratio is thus 20 dB.)

The reference space-time field was synthesized by the Fourier transform of random amplitudes and phases. High frequencies were cut out to produce smooth fields. However, as mentioned earlier, no regularity assumption was exploited to retrieve the modes. Thus, this regularity is more relevant to pinpoint unsatisfactory recovery from visual inspection.

For the approach to make sense, some redundancy is necessary, and hence the reference data should require less data than the measured ones. Hence, it was chosen to consider only $N_{\text{mode}} = 4$ separated modes. Each mode requires $(N_x + N_t)$ components. Therefore (when the measurements are homogeneous in the space-time domain), the redundancy is

$$\beta = \frac{\text{Measurements}}{\text{Information content}} = \frac{\eta N_x N_t}{N_{\text{mode}}(N_x + N_t)} = 1.28 \tag{17}$$

so that no more than 28% of the data is redundant and is to be used to reduce noise. The three cases of distribution of measurements in space and time that are shown in Fig. 1 were tested together with a completely random distribution of measurements, but the subsampling was kept at a constant value $\eta = 1\%$.

In order to evaluate the proposed algorithm a comparison is proposed with the two reference algorithms discussed earlier, GPOD1 and GPOD2. All algorithms are iterative, and hence the same criterion was chosen to terminate the iterative procedure. When the increment in relative error between two successive iteration became smaller than 10^{-4}, iterations were stopped. Hence the number of iterations varies from one case to the other. Moreover, the maximum number of iterations was set to a maximum value of 400 if the previous criterion was not reached. However, because both GPOD2 and the proposed algorithm involve many loops, their total number of iterations (summed over all loops) may exceed 400.

In Table 1, the results of the four different cases illustrated in Fig. 1 for all three algorithms are reported. The final error is computed as the norm (over space and time) of the difference between the recovered field, and the original reference field without noise. This norm is scaled to the standard deviation of the original reference field. The presence of a high level of noise and of the very sparse acquisition $\eta = 1\%$ is such that the computation cannot recover exactly the original data.

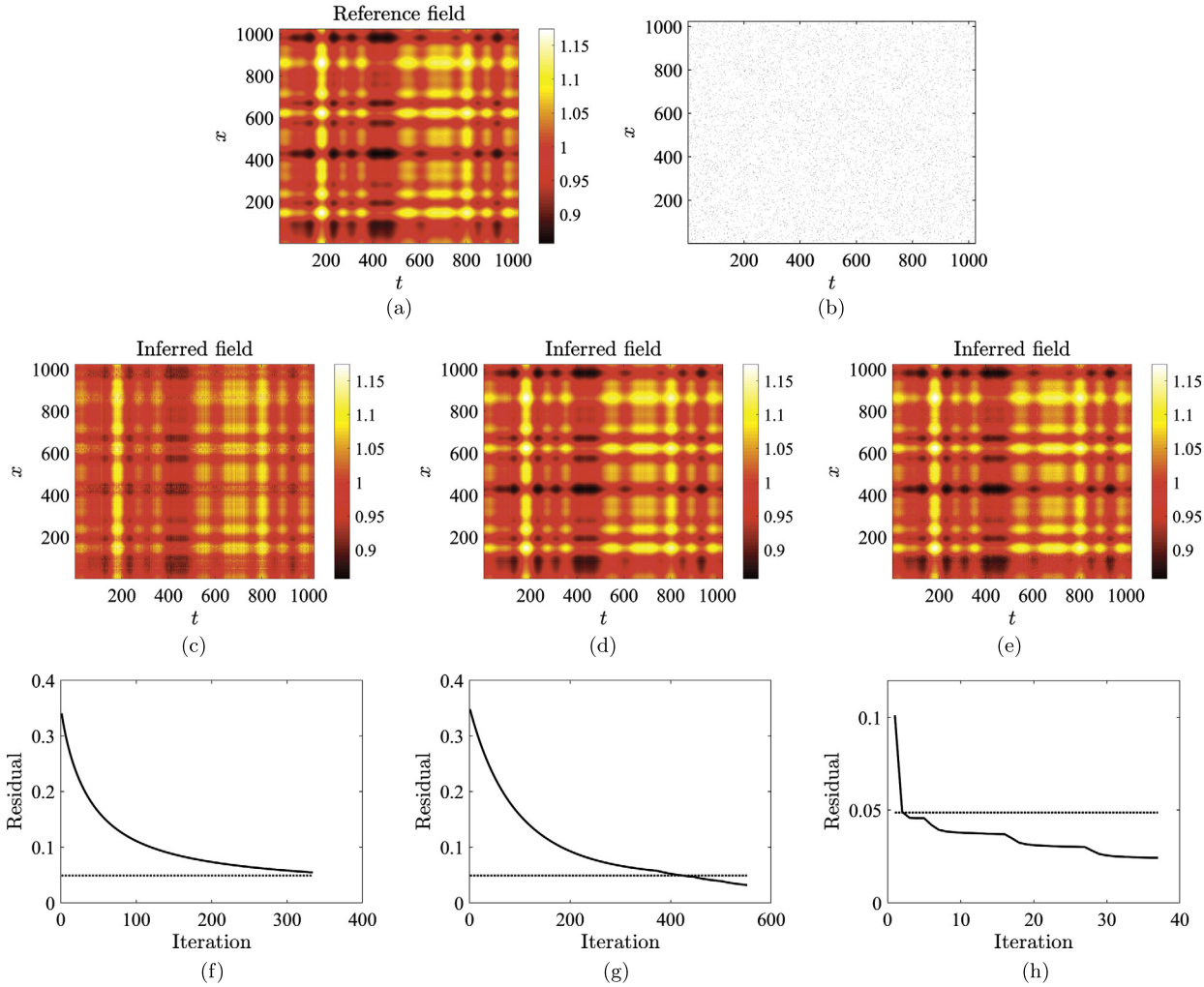

Fig. 2. Random acquisition case. (a) Reference field; (b) measurement support with random acquisitions; (c) reconstructed field using GPOD1; (d) reconstructed field using GPOD2; (e) reconstructed field using the proposed method; (f) relative error between reconstruction and reference as a function of iteration number for GPOD1; (g) same relative error for GPOD2; (h) same relative error for the proposed method.

The sole presence of noise would be responsible for an error of about 4 to 5%. The exploitation of the presence of only few modes, allows all algorithms to reduce this error to a lower level in all cases. However, all algorithms do not reach the same level of final error. Both variants of Gappy-POD provide results of comparable quality in terms of errors, but GPOD2 requires often more iterations than GPOD1, so that the claimed benefit of a progressive enrichment of modes does not appear so obvious in the studied case (which is clearly an extreme case). The proposed method shows generally a markedly lower residual error (down to 50% smaller), and yet with a much lower number of iterations.

Two cases are chosen for a more detailed illustration, the random acquisition case in Fig. 2 and the continuous scan in Fig. 3. In both figures, the reference field (without noise) is shown on the top line together with the support of the measurement. The fields reconstructed from the four identified modes are displayed for the three algorithms. Finally, the evolution of the error with iterations is shown for the three algorithms. The fact that both GPOD2 and the proposed method consists of $N_{\text{mode}} = 4$ loops can be seen from the error evolution. In this latter set of graph, the error that would correspond only to the presence of noise (but no missing data, and no mode recovery treatment) is indicated as a dotted line. It is to be noted that the range of variation of both axes differ from one algorithm to the next.

In Fig. 2, GPOD1 shows a marked dissymmetry between time where the mode are well captured and space where amplitudes are depressed. It is also to be noted that convergence is quite slow, and the criterion for interrupting the mode recovery stopped the computation well before its asymptotic result. GPOD2 performs much better for the reconstructed field, but required more than 200 additional iterations. The proposed algorithm has a residual error level better than that of noise after only 2 iterations (to be compared to 450 for GPOD1, and 420 for GPOD2).

In Fig. 3, relative to the “continuous scan” case, the temporal evolution is well captured, but the spatial modes seem to have been erased, for both GPOD1 and GPOD2. (This dissymmetry between space and time originates from the way missing

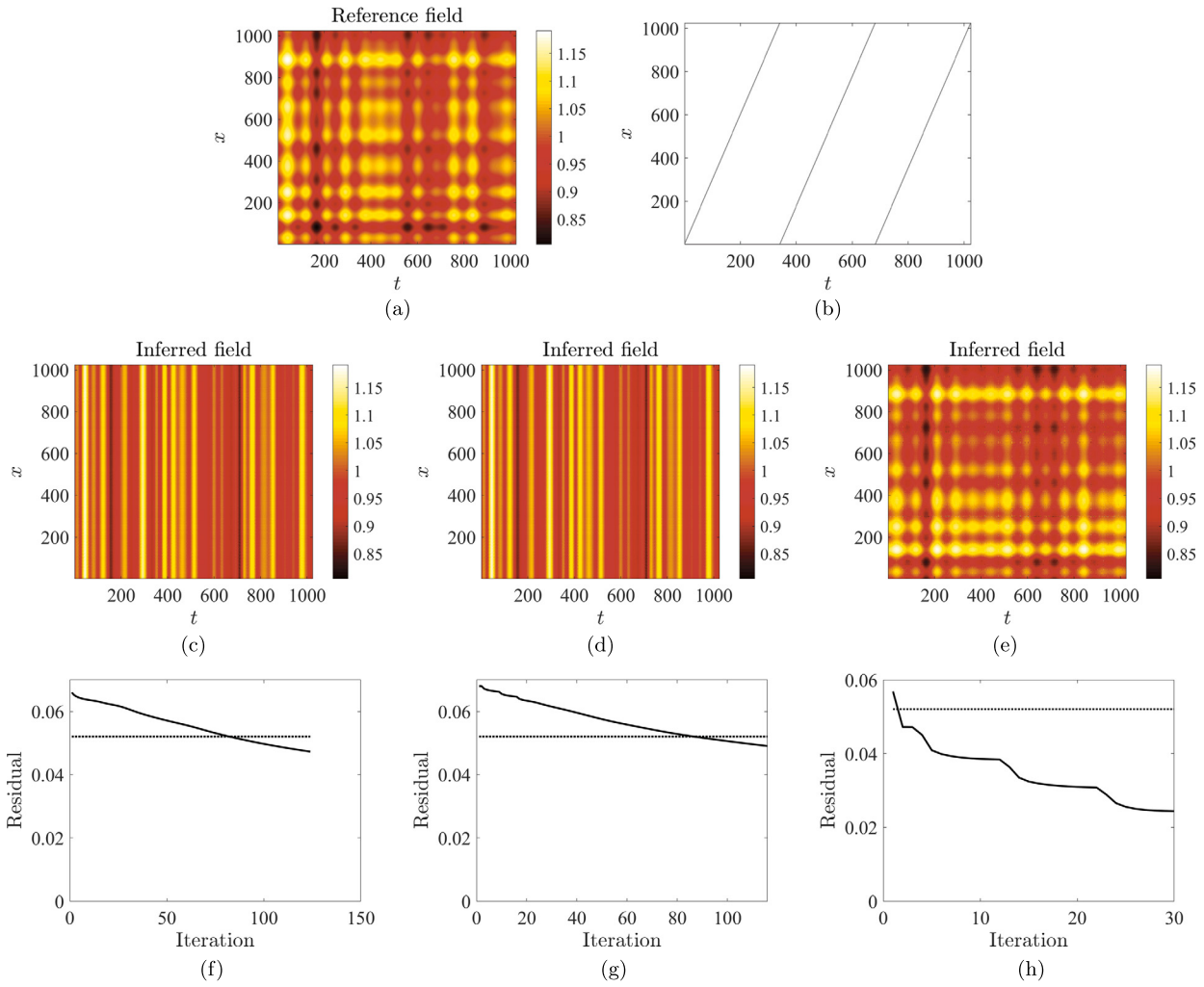

Fig. 3. Continuous scan case. (a) Reference field; (b) measurement support; (c) reconstructed field using `GPOD1`; (d) reconstructed field using `GPOD2`; (e) reconstructed field using the proposed method; (f) relative error between reconstruction and reference as a function of iteration number for `GPOD1`; (g) same relative error for `GPOD2`; (h) same relative error for the proposed method.

data are filled in with *spatial* averages at each instant of time.) This is to be contrasted with the present method, which gives a much more balanced picture of the space-time field, and reaches an error level that is cut down by a factor of 2 as compared to Gappy-POD results. For all three algorithms, convergence is faster than for the previous "random" case, and the convergence criterion is reached much earlier in terms of iterations.

5. Conclusion

The present paper has introduced a new algorithm to handle Proper Orthogonal Decomposition (POD, or PCA) for partial measurement. This algorithm, when tested over examples of very sparse data acquisition, and very noisy data, was observed to outperform different variants of Gappy-POD, in terms of result quality and convergence speed.

The very formulation of the introduced algorithm makes its extension to Proper Generalized Decomposition (PGD) straightforward. Namely, the cost function that was used herein, Eq. (8), involves a simple L2 norm, but can simply be tailored to any other problems where a variational formulation is accessible.

Acknowledgements

The authors acknowledge the support of Safran Tech for a project where the above procedure extended to Digital Volume Correlation was applied successfully. This work benefitted from useful discussions with N. Belkhir, D. Duclos, E. Parra, and J. Schneider.

References

[1] M.A. Sutton, W.J. Wolters, W.H. Peters, W.F. Ranson, S.R. McNeill, Determination of displacements using an improved digital correlation method, Image Vis. Comput. 1 (3) (1983) 133–139.
[2] M.A. Sutton, J.J. Orteu, H. Schreier, Image Correlation for Shape, Motion and Deformation Measurements: Basic Concepts, Theory and Applications, Springer Science & Business Media, 2009.
[3] B.K. Bay, T.S. Smith, D.P. Fyhrie, M. Saad, Digital volume correlation: three-dimensional strain mapping using x-ray tomography, Exp. Mech. 39 (3) (1999) 217–226.
[4] G. Besnard, S. Guérard, S. Roux, F. Hild, A space–time approach in digital image correlation: movie-dic, Opt. Lasers Eng. 49 (1) (2011) 71–81.
[5] A. Buljac, C. Jailin, A. Mendoza, J. Neggers, T. Taillandier-Thomas, A. Bouterf, B. Smaniotto, F. Hild, S. Roux, Digital volume correlation: review of progress and challenges, Exp. Mech. 58 (5) (2018) 661–708.
[6] R.A. Newcombe, A.J. Davison, Live dense reconstruction with a single moving camera, in: 2010 IEEE Computer Society Conference on Computer Vision and Pattern Recognition, IEEE, 2010, pp. 1498–1505.
[7] S.J. Rothberg, M.S. Allen, P. Castellini, D. Di Maio, J.J.J. Dirckx, D.J. Ewins, J. Ben Halkon, P. Muyshondt, N. Paone, T. Ryan, et al., An international review of laser doppler vibrometry: making light work of vibration measurement, Opt. Lasers Eng. 99 (2017) 11–22.
[8] J.E. Dufour, F. Hild, S. Roux, Shape, displacement and mechanical properties from isogeometric multiview stereocorrelation, J. Strain Anal. Eng. Des. 50 (7) (2015) 470–487.
[9] M. Berny, T. Archer, A. Mavel, P. Beauchêne, S. Roux, F. Hild, On the analysis of heat haze effects with spacetime dic, Opt. Lasers Eng. 111 (2018) 135–153.
[10] M.A. Iadicola, Uncertainties of Digital Image Correlation Due to Pattern Degradation at Large Strain, Advancement of Optical Methods in Experimental Mechanics, vol. 3, Springer, 2016, pp. 247–253.
[11] H. Leclerc, S. Roux, F. Hild, Projection savings in ct-based digital volume correlation, Exp. Mech. 55 (1) (2015) 275–287.
[12] C. Jailin, A. Buljac, A. Bouterf, F. Hild, S. Roux, Fast 4d tensile test monitored via X-CT: single projection based digital volume correlation dedicated to slender samples, J. Strain Anal. Eng. Des. 53 (7) (2018) 473–484.
[13] J. Neggers, O. Allix, F. Hild, S. Roux, Big data in experimental mechanics and model order reduction: today's challenges and tomorrow's opportunities, Arch. Comput. Methods Eng. 25 (1) (2018) 143–164.
[14] P. Netrapalli, U.N. Niranjan, S. Sanghavi, A. Anandkumar, P. Jain, Non-convex robust pca, in: Advances in Neural Information Processing Systems, 2014, pp. 1107–1115.
[15] F. Wen, L. Chu, P. Liu, R.C. Qiu, A survey on nonconvex regularization-based sparse and low-rank recovery in signal processing, statistics, and machine learning, IEEE Access 6 (2018) 69883–69906.
[16] F. Mathieu, H. Leclerc, F. Hild, S. Roux, Estimation of elastoplastic parameters via weighted femu and integrated-dic, Exp. Mech. 55 (1) (2015) 105–119.
[17] A. Buljac, M. Shakoor, J. Neggers, M. Bernacki P-O Bouchard, L. Helfen, T.F. Morgeneyer, F. Hild, Experimental-numerical validation framework for micromechanical simulations, in: Multiscale Modeling of Heterogeneous Structures, Springer, 2018, pp. 147–161.
[18] C. Jailin, A. Buljac, A. Bouterf, F. Hild, S. Roux, Fast four-dimensional tensile test monitored via x-ray computed tomography: elastoplastic identification from radiographs, J. Strain Anal. Eng. Des. 54 (1) (2019) 44–53.
[19] R.G. Baraniuk, Compressive sensing, IEEE Signal Process. Mag. 24 (4) (2007).
[20] M.F. Duarte, M.A. Davenport, D. Takhar, J.N. Laska, T. Sun, K.F. Kelly, R.G. Baraniuk, Single-pixel imaging via compressive sampling, IEEE Signal Process. Mag. 25 (2) (2008) 83–91.
[21] R. Everson, L. Sirovich, Karhunen–Loève procedure for gappy data, J. Opt. Soc. Amer. A 12 (8) (1995) 1657–1664.
[22] K. Willcox, Unsteady flow sensing and estimation via the gappy proper orthogonal decomposition, Comput. Fluids 35 (2) (2006) 208–226.
[23] N.E. Murray, L.S. Ukeiley, An application of gappy pod, Exp. Fluids 42 (1) (2007) 79–91.
[24] J.-C. Passieux, J.-N. Périé, High resolution digital image correlation using proper generalized decomposition: PGD-DIC, Int. J. Numer. Methods Eng. 92 (6) (2012) 531–550.
[25] M. Berny, C. Jailin, A. Bouterf, F. Hild, S. Roux, Mode-enhanced space-time dic: applications to ultra-high-speed imaging, Meas. Sci. Technol. 29 (12) (2018) 125008.
[26] P. Ladevèze, Nonlinear Computational Structural Mechanics: New Approaches and Non-Incremental Methods of Calculation, Springer Science & Business Media, 2012.
[27] L.G. Perini, J.C. Passieux, J.N. Périé, A multigrid pgd-based algorithm for volumetric displacement fields measurements, Strain 50 (4) (2014) 355–367.
[28] A.B. Stanbridge, D.J. Ewins, Modal testing using a scanning laser doppler vibrometer, Mech. Syst. Signal Process. 13 (2) (1999) 255–270.
[29] C. Jailin, T. Jailin, S. Roux, Measurement of 1–10 Hz 3D vibration modes with a CT-scanner, preprint, 2019.
[30] J.M. Beckers, M. Rixen, Eof calculations and data filling from incomplete oceanographic datasets, J. Atmos. Ocean. Technol. 20 (12) (2003) 1839–1856.
[31] C. Jailin, Full field modal measurement with a single standard camera, Opt. Lasers Eng. 107 (2018) 265–272.